MZ-ETAP/89-4
May 1989

JOHANNES GUTENBERG-UNIVERSITÄT MAINZ
Fachbereich Physik
Institut für Physik

Observation of an Isoscalar Meson AX(1565) in Annihilation of the $\bar{p}p$-Atom from P States

B. May, K.D. Duch[1], M. Heel[2], H. Kalinowsky, F. Kayser[3], E. Klempt, J. Reifenröther, O. Schreiber[4], P. Weidenauer, M. Ziegler[5]
Institut für Physik, Johannes-Gutenberg-Universität, 6500 Mainz, Germany

D. Bailey[6], S. Barlag[7], J.M. Butler[8], U. Gastaldi[9], R. Landua[9], C. Sabev
CERN, 1211 Genève, Switzerland

W. Dahme[10], F. Feld-Dahme[11], U. Schaefer[12], W.R. Wodrich[1,9]
Sektion Physik, Ludwig-Maximilians-Universität, 8000 München, Germany

J.C. Bizot, B. Delcourt, J. Jeanjean, H. Nguyen
Laboratoire de l'Accélérateur Linéaire, Université de Paris-Sud, 91405 Orsay, France

E.G. Auld, D.A. Axen, K.L. Erdman, B. Howard, R. Howard, B.L. White
Department of Physics, University of British Columbia, Vancouver, B. C., Canada V6T2A6

S. Ahmad, M. Comyn, G.M. Marshall
TRIUMF, Vancouver, B. C., Canada V6T2A3

G. Beer, L.P. Robertson
Department of Physics, University of Victoria, Victoria, B. C., Canada V8W2Y2

M. Botlo[13], C. Laa[14], H. Vonach
Institut für Kernphysik, Universität Wien, 1090 Wien, Austria

C. Amsler, M. Doser[15], J. Riedlberger, U. Straumann[9], P. Truöl
Physik Institut der Universität Zürich, 8001 Zürich, Switzerland

ASTERIX Collaboration

May 18, 1989

[1] present address: Schott Glaswerke, 6500 Mainz/Wiesbaden, Germany
[2] present address: Boehringer, 6507 Ingelheim, Germany
[3] present address: Volkshochschule, 6450 Hanau, Germany
[4] present address: AT+T, 8000 München, Germany
[5] present address: GEI, 6100 Darmstadt, Germany
[6] present address: University of Toronto, Ontario, Canada M5S1A7
[7] present address: Max Planck Institut, 8000 München, Germany
[8] present address: FNAL, Batavia, Illinois, USA 60510
[9] part of this work was done while at Universität Mainz
[10] present address: LeCroy Research Systems, 1211 Genève, Switzerland
[11] present address: CERN, 1211 Genève, Switzerland
[12] present address: DLR, 7000 Stuttgart, Germany
[13] present address: Österreichische Akademie der Wissenschaften, 1050 Wien, Austria
[14] present address: Voest Alpine, 1050 Wien, Austria
[15] present address: KEK, Tsukuba 305, Japan

submitted to Physics Letters B

Abstract

A new isoscalar $\pi\pi$ resonance AX(1565) has been observed at a mass of 1565±10 MeV/c^2 and a width of 170±20 MeV/c^2. The resonance is produced in $\bar{p}p$ annihilation at rest into $\pi^+\pi^-\pi^0$ from P states of antiprotonic hydrogen atoms formed by stopping antiprotons in hydrogen gas at normal temperature and pressure. Annihilation from P states is identified by coincident observation of the L X-ray series emitted in the cascade of $\bar{p}p$ atoms. The resonance is seen as striking peak in the $\pi^+\pi^-$ invariant mass spectrum. The phase of the $\pi^+\pi^-$ D wave shows a resonance-like behaviour. Hence we assign the quantum numbers $I^G(J^{PC})$=$0^+(2^{++})$ to the resonance.

We have observed a new resonance at a mass of (1565±10) MeV/c^2 and a width of (170±20) MeV/c^2 decaying into $\pi^+\pi^-$. The resonance is produced in $\bar{p}p$ annihilation from P states of antiprotonic hydrogen atoms into the final state $\pi^+\pi^-\pi^0$. Initial and final states are identified in a magnetic spectrometer which allows to detect low-energy X-rays emitted in the cascade of $\bar{p}p$ atoms in coincidence with charged particles produced in the annihilation process. The detector was designed [1] to allow identification of the initial [2] and the final [3] state in $\bar{p}p$ annihilation at rest, since it was expected that the production of meson resonances with higher spins should be enhanced in annihilation from P states [1]. This might have led to the chance to observe narrow states which were predicted [4] when this experiment was initiated. However, early searches for narrow resonances possibly produced in $\bar{p}p$ annihilation at rest yielded only negative results, not only for annihilation from S states [5], but also for annihilation from P states [6].

Changing the fraction of S wave and P wave annihilation for a particular final state is a decisive new tool for finding the resonance reported here. Annihilation from S states is dominant when antiprotons are stopped in liquid H_2 [7]. These antiprotons form antiprotonic hydrogen atoms which experience intense electric fields when colliding with neighbouring H_2 molecules. This leads to a reshuffling of the populations of levels with different angular momenta, and annihilation from S states is possible already in highly excited states [8]. This mechanism is less effective in H_2 gas at normal temperature and pressure (NTP). The cascade process is slower [9], radiative transitions to the low-lying atomic levels of the $\bar{p}p$ atoms become possible [10], and annihilation from P states contributes significantly.

The fraction of S wave and P wave annihilation of antiprotons stopping in gaseous hydrogen at NTP was determined in this experiment. The branching ratios for $\bar{p}p$ annihilation into K^+K^- and $K^0\overline{K^0}$ were measured in liquid H_2, gaseous H_2 and in coincidence with radiative transitions to the 2P levels of the antiprotonic hydrogen atoms[11]. These branching ratios depend strongly on the fraction of S and P wave. In H_2 gas a (52.8±4.9)% fraction of P wave annihilation was determined[11]. This fraction can be enhanced by selecting events in which a low-energetic X-ray emitted in the cascade of the $\bar{p}p$ atom is detected in coincidence with the final state. These X-rays are mostly L X-rays populating the 2P levels of the $\bar{p}p$ atom from which annihilation is known [10] to prevail. Bremsstrahlung emitted by the sudden acceleration of charged particles in the annihilation process is an unavoidable background. However, this process can be calculated [12]. It leads to a (7±2)% contamination of the $\pi^+\pi^-\pi^0$ data sample with annihilations from S states.

For the present analysis we have taken 120 000 events of the type $\bar{p}p \rightarrow \pi^+\pi^-\pi^0$. Of these, 40 000 were taken without requiring X-rays. We call these data $\bar{p}$-GAS data. A sample of 80 000 events were taken with a special trigger asking for X-ray candidates. The latter data sample is scanned for detection of a true low-energy X-ray. This results in 19 735 events called $\bar{p}$-LX data. From these two data sets we derive the dynamics of $\bar{p}p$ annihilation into $\pi^+\pi^-\pi^0$ from S states and from P states. Details of the analysis method and the full results are given in a forthcoming publication [13]. Here we present only those results which are related to the observation of the new meson resonance.

The data were taken with the ASTERIX spectrometer [15] at the Low Energy Antiproton Ring (LEAR) at CERN. A beam of 105 MeV/c antiprotons with an intensity of a few 10 000 $\bar{p}$/s traversed an entrance scintillator of 50 μm thickness defining a START signal. Nearly all antiprotons stopped in a fiducial volume which was completely contained in the H_2 gas target at NTP, 80 cm in length and 16 cm in diameter. The target was surrounded by a X-ray drift chamber (XDC)[16] and separated from it by an aluminized mylar membrane of

6 μm thickness. The XDC detected with a solid angle of ~90% of 4π X-rays associated with antiprotons stopping in the H_2 target. The XDC was also used to track the innermost space points of charged particles produced in $\bar{p}p$ annihilation.

The XDC was surrounded by seven cylindrical multiwire proportional chambers. Helical cathode readout on five of these chambers allowed to reconstruct tracks of charged particles in three dimensions. A magnetic field of 0.8 Tesla allowed to measure the momenta of charged particles. For long tracks reaching one of the outermost chambers the momentum resolution of the spectrometer was

$$\frac{\sigma_p}{p} = \left[(0.042p)^2 + 0.023^2\right]^{1/2}, \qquad p \text{ in } GeV/c\,. \tag{1}$$

Gammas were converted in a lead foil in front of the last two chambers and in lead foils at both endplates of the solenoidal magnet. Gamma detection was not used for the present analysis. For the present data a trigger on two long tracks was required which led to a momentum cut-off at 100 MeV/c and reduced the geometrical acceptance for charged particles to 2π sr. However, it allowed the best momentum resolution achievable with the ASTERIX detector.

Fig. 1 shows the missing mass squared distribution recoiling against two charged particles. Peaks due to π^0's, η's or ω's are seen which originate from the neutral decay modes of η or ω. The data were kinematically fitted to the $\pi^+\pi^-\pi^0$ hypothesis; events passing this fit with a probability of more than 1% still contain a large fraction of background events. To reduce this background, only events with a fit probability greater than 10% for the three pion hypothesis are used in the following analysis. The probability distribution of the kinematical fit is shown as an inset in Fig. 1. The background is estimated to be (8±4)%.

The Dalitz plot of the 19 735 $\pi^+\pi^-\pi^0$ events observed in coincidence with a low-energy X-ray (<4 keV) is shown in Fig. 2. Clear bands due to the production of charged and neutral $\varrho(770)$ mesons and of $f_2(1270)$ mesons are seen. In addition, a weak band in the lower left corner of the Dalitz plot is observed. The band corresponds to a peak in $\pi^+\pi^-$ mass spectrum associated with $\bar{p}p$ annihilation from P states. A partial wave analysis of the Dalitz plot was made by comparing the experimental Dalitz plot with a sum of Monte Carlo generated Dalitz plots. These Dalitz plots describe annihilation from the three $\bar{p}p$ states with quantum numbers ${}^{3S+1}L_J = {}^1P_1$, ${}^3P_1$, and ${}^3P_2$ where S denotes the spin of the $\bar{p}p$ atom and J the total angular momentum. (Annihilation into $\pi^+\pi^-\pi^0$ from the ${}^3P_0$ state is forbidden.) Each initial state annihilates into $\pi^+\pi^-\pi^0$ via interfering amplitudes. The amplitudes are defined as a product of Clebsch-Gordan coefficients, of Zemach tensors [14] describing the angular distributions, and, in case of resonances, of a dynamical factor, which is given by a relativistic Breit-Wigner amplitude of the form

$$\left(\frac{m}{q}\right)^{\frac{1}{2}} \frac{\Gamma(m)^{\frac{1}{2}}}{(m_0{}^2 - m^2) - im_0\Gamma(m)} \tag{2}$$

with

$$\Gamma(m) = \Gamma_0 \left(\frac{q}{q_0}\right)^{2l+1} \frac{\rho(m)}{\rho(m_0)}$$

m_0, q_0 are mass and decay momentum at the center of the resonance. Different functions $\rho(m)$ are used in the literature [15]. We find no significant differences and use $\rho(m) = 1/m$. Phase space distributed Monte Carlo events were filled into Dalitz plots with the squared amplitudes as weights. The comparison between data and generated Dalitz plots was made by a χ^2 test.

The Dalitz plot was divided into 0.2×0.2 GeV^2/c^4 mass squared bins and folded around the diagonal in order to increase the statistics per cell.

Fig. 3 shows the $\pi^+\pi^-$ invariant mass spectrum. Apart from the $\varrho^0(770)$ and the $f_2(1270)$ there is clear evidence for a third peak which we call AX(1565). By fitting the spectrum with two relativistic Breit-Wigner functions for the $f_2(1270)$ and the AX(1565) and a background function we obtain mass and width of the AX(1565)

$$\begin{aligned} M &\doteq (1565 \pm 10)\ \mathrm{MeV/c^2} \\ \Gamma &= (\ 170 \pm 20)\ \mathrm{MeV/c^2} \end{aligned}$$

The background function is obtained by a partial wave analysis of the low mass part of the Dalitz plot ($m^2(\pi^+\pi^-)<0.8\,\mathrm{GeV^2/c^4}$). We have investigated four possible origins which might be responsible for this peak:

i) Background due to events $\bar{p}p \rightarrow \pi^+\pi^-\eta$ or $\pi^+\pi^-\pi^0\pi^0$ passing the kinematical fit to the $\pi^+\pi^-\pi^0$ hypothesis:

We have studied those events which pass the kinematical $\pi^+\pi^-\pi^0$ fit with a probability between 1% and 10%. These events fill preferentially the upper and the lower right corner of the Dalitz plot for which the momentum of the faked π^0 and one of the charged particles is high. The region of high $\pi^+\pi^-$ invariant masses is nearly free of any background contamination. This is confirmed by Monte Carlo simulations of events $\pi^+\pi^-\eta$ and $\pi^+\pi^-\pi^0\pi^0$. Hence the AX(1565) is not produced by background events.

ii) Increase of acceptance at high $\pi^+\pi^-$ invariant masses:

If two charged particles are emitted back to back, then the acceptance of our spectrometer is 50%: the detection of the first charged particle entails the geometrical acceptance of the second track. For two uncorrelated pions, the acceptance of our 2π sr detector is, however, only 25%. Hence the acceptance of the spectrometer is higher in the AX(1565) mass region than in the $\varrho^0(770)$ mass region. Of course, the acceptance can be taken into account by Monte Carlo simulations; but the accuracy of the Monte Carlo simulations needs to be verified. We have therefore fitted the Dalitz plot of the $\bar{p}$-GAS data with the experimental Dalitz plot of $\bar{p}$-LX data and a superposition of Monte Carlo Dalitz plots simulating annihilations from S states. The results of this fit, described in ref.[13], are the fraction of S and P wave annihilation, and parameters describing annihilation from S states.

Annihilation into $\pi^+\pi^-\pi^0$ from S states had been studied more than 20 years ago in a bubble chamber [17]. The process was described by annihilation from S states of the $\bar{p}p$ atom, characterized by their quantum numbers $I^G(J^{PC})$. These are the isospin I, the G-parity, the total spin J, the parity P and charge conjugation parity C. The following reaction modes were considered:

$$\begin{aligned} \bar{p}p\ (1^-(0^{-+})) &\rightarrow \pi^+\pi^-\pi^0 & &\text{phase space} & (3a)\\ &\rightarrow f_2(1270)\pi^0 & &(l=2) & (3b)\\ &\rightarrow \varrho^\pm(770)\pi^\mp & &(l=1) & (3c) \end{aligned}$$

$$\begin{aligned} \bar{p}p\ (0^-(1^{--})) &\rightarrow \varrho^\pm(770)\pi^\mp,\ \varrho^0(770)\pi^0 & &(l=1) & (4a)\\ &\rightarrow \pi^+\pi^-\pi^0 & &\text{phase space} & (4b) \end{aligned}$$

The variable l denotes the angular momentum between the dipion resonance and the third pion. The amplitudes describing annihilation from one $\bar{p}p$ initial state were added coherently, those describing annihilation from different $\bar{p}p$ initial states incoherently.

The same parametrization was used for our fit. In addition we imposed a background Dalitz plot derived from events with low probability (1%–10%) under the $\pi^+\pi^-\pi^0$ hypothesis. The results obtained in our experiment were compared to the bubble chamber results. All amplitudes and phases determined in these two very different experiments agree within one standard deviation [13]. This shows that the detector acceptance and efficiency are described correctly.

iii) Coherent interference of $\varrho^+(770)$ and $\varrho^-(770)$ amplitudes:

The two amplitudes for production of charged $\varrho^\pm(770)$ mesons interfere in the region of the Dalitz plot in which the $\pi^+\pi^-$ invariant mass is high (Fig. 3). The interference increases the number of events in parts of the Dalitz plot and may thus produce a peak in the neutral dipion system. In order to check this hypothesis we have performed fits to the Dalitz plot using amplitudes for the following reactions:

$$\begin{aligned} \bar{p}p\ (0^-(1^{+-})) &\rightarrow \varrho^\pm(770)\pi^\mp,\ \varrho^0(770)\pi^0 && (l=0) && \text{(5a)}\\ &\rightarrow \varrho^\pm(770)\pi^\mp,\ \varrho^0(770)\pi^0 && (l=2) && \text{(5b)}\\ &\rightarrow \pi^+\pi^-\pi^0 && \text{phase space} && \text{(5c)} \end{aligned}$$

$$\begin{aligned} \bar{p}p\ (1^-(1^{++})) &\rightarrow \varrho^\pm(770)\pi^\mp && (l=0) && \text{(6a)}\\ &\rightarrow f_2(1270)\pi^0 && (l=1) && \text{(6b)}\\ &\rightarrow \pi^+\pi^-\pi^0 && \text{phase space} && \text{(6c)} \end{aligned}$$

$$\begin{aligned} \bar{p}p\ (1^-(2^{++})) &\rightarrow \varrho^\pm(770)\pi^\mp && (l=2) && \text{(7a)}\\ &\rightarrow f_2(1270)\pi^0 && (l=1) && \text{(7b)}\\ &\rightarrow \pi^+\pi^-\pi^0 && \text{phase space} && \text{(7c)} \end{aligned}$$

Initial states with Isospin $I = 0$ allow annihilation into $\varrho^0(770)\pi^0$ while this reaction is forbidden from $I = 1$ initial states. Note that the negative G parity of the 3π system fixes the isospin component of a $\bar{p}p$ atomic level since $G = (-1)^{L+S+I}$. In addition to these amplitudes from which Monte Carlo Dalitz plots are constructed we imposed a Dalitz plot representing the 7% of $\bar{p}p$ annihilations from S states and a Dalitz plot representing the background.

The result of the fit is presented in Fig. 4a by comparing the $\pi^+\pi^-$ invariant mass spectrum and the fit result (solid line). Obviously the description is rather poor in the high mass region; a large fraction of the χ^2 of 599 (for 266 degrees of freedom) is due to this mass region. Therefore we have limited the fit to the region of the Dalitz plot for which the $\pi^+\pi^-$ invariant mass is smaller than 1.31 GeV/c^2 and have extrapolated the fit into the high mass region (Fig. 4b). This procedure is possible since the ratio of charged $\varrho^\pm(770)$ and neutral $\varrho^0(770)$ completely defines the contributions of constructive and destructive interference between the two charged $\varrho^\pm(770)$ mesons; the contributions of $\varrho^\pm(770)$ and $\varrho^0(770)$ mesons can confidently be derived from the reduced Dalitz plot. The extrapolation shows an additional count rate at high masses wich is not accounted for by ϱ interference effects. Fig. 4c shows the $\pi^\pm\pi^0$ invariant mass and the result of the fit using the reduced Dalitz plot. The missing events are distributed over a wide mass range and not concentrated at the $\varrho^\pm(770)$ peak. A concentration of the missing intensity at the peak of the $\varrho^\pm(770)$ would be expected, if the peak at 1565 MeV/c^2 should originate from a wrong description of the $\varrho^{\pm}(770)$ interference. We conclude that the AX(1565) cannot be attributed to the ϱ^+–ϱ^- interference.

iv) Production of a new resonance:

We have tested the hypothesis that the AX(1565) is a genuine resonance. In this case it must be isoscalar since charged partners are not observed. If it would be an isovector resonance, the charged partners would need to be produced with the same rate as the AX(1565); a I=2 resonance would decay into charged and neutral dipions with a ratio of 3/4. Both hypotheses are incompatible with Fig. 4c. Hence its quantum numbers are even (0^{++}, 2^{++}; 4^{++}, ...). Selection rules then limit the possible annihilation modes in which the resonance is produced to the following reactions:

If the AX(1565) is $J = 2$:

$$\bar{p}p\ (1^-(1^{++})) \rightarrow \mathrm{AX}(1565)\pi^0 \qquad (l = 1) \qquad (6d)$$
$$\bar{p}p\ (1^-(2^{++})) \rightarrow \mathrm{AX}(1565)\pi^0 \qquad (l = 1) \qquad (7d)$$

If the AX(1565) is $J = 0$:

$$\bar{p}p\ (1^-(1^{++})) \rightarrow \mathrm{AX}(1565)\pi^0 \qquad (l = 1) \qquad (6d')$$

To test the resonance interpretation and to determine the spin of the AX(1565) we defined eight mass squared strips in the Dalitz plot, from 2.1 to 3.0 $\mathrm{Gev}^2/\mathrm{c}^4$ and with a width of 0.2 $\mathrm{Gev}^2/\mathrm{c}^4$. Overlapping strips were chosen since the statistics per strip is rather low. We used these strips for eight consecutive fits in which the data of the reduced Dalitz plot (with $m^2(\pi^+\pi^-) < 1.7\,\mathrm{GeV}^2/\mathrm{c}^4$) and those of one mass strip were fitted. For these fits we used fixed amplitudes defined by the fit on the reduced Dalitz plot, and one complex amplitude to describe the AX(1565) in one mass bin. The complex amplitude was alternatively chosen to describe a 0^{++} or 2^{++} angular distribution. The modulus of the amplitude and the phase were allowed to adjust themself to describe the extra intensity in Fig. 4b. This phase as a function of the $\pi^+\pi^-$ invariant mass is shown in Fig. 5a,b. for both hypotheses. The solid lines represent the phase motions which would be expected from a $\pi^+\pi^-$ resonance at a mass of 1565 $\mathrm{MeV}/\mathrm{c}^2$ and a width of 170 $\mathrm{MeV}/\mathrm{c}^2$. The 0^{++} hypothesis does not show a resonance-like behaviour. A fit to the data with one parameter, the offset of the phase, gives a χ^2 of 74.4 for 7 d.o.f.. The 2^{++} hypothesis is fully compatible with a resonance interpretation (χ^2/d.o.f.=8.2/7).

We conclude that the AX(1565) represents a true resonance which should be taken into account as a normal Breit Wigner resonance for the final fit. The phase shift analysis suggests strongly that the AX(1565) is $J = 2$. However, the angular distribution (Fig. 6f) does not allow to determine the spin unambiguously because of strong distortions by the ϱ^+-ϱ^- interference. Notice that there is no evidence for the AX(1565) in $\bar{p}p$ annihilation from S states of the $\bar{p}p$ atom. Figure 4d shows the $\pi^+\pi^-$invariant mass spectrum of the $\bar{p}$-GAS data which contains approximately 50% of S wave annihilation. The AX(1565) peak is suppressed by about a factor of two. Also, there was no evidence for the AX(1565) in the bubble chamber data [17].

The final partial wave analysis was performed using amplitudes for reactions (5–7,a–d), with J^{PC}=2^{++} for the AX(1565). The results of the fit are compared to the experimental data in Fig. 6a-f. Mass distributions and angular distributions are reasonably well described by the fit. The χ^2 is now 427. This is still rather high but an improvement by 167 χ^2 units in comparison to the fit without the AX(1565). The main reasons for the still too large χ^2 are the poor description of the $\varrho^0(770)$ produced from the $0^-(1^{+-})$ $\bar{p}p$ atomic state. Its mass appears to be shifted to higher masses, an effect which is not accounted for by the amplitudes (6). The fit is, however, good in the high mass region. The absolute branching ratio for $\bar{p}p \to \pi^0$AX(1565), AX(1565) $\to \pi^+\pi^-$ is $(3.7 \pm 0.6)\cdot 10^{-3}$.

If the AX(1565) is assumed to have spin zero (amplitude (6e)) the χ^2 increases by 35 units to 462. This χ^2 difference does not allow to establish firmly the spin of the AX(1565), even though $J^{PC}=2^{++}$ is deduced from the phase motions.

There are two more arguments, favouring a $J^{PC}= 2^{++}$ over 0^{++} for the AX(1565): The first argument is the similarity of the production mechanisms for the $f_2(1270)$ and the AX(1565). The $f_2(1270)$ is produced very weakly from the $1^-(0^{-+})$ $\bar{p}p$ initial state, strongly produced from the $1^-(1^{++})$ state, and some production is observed from the $1^-(2^{++})$ initial state. The AX(1565) follows the same pattern, no production from $1^-(0^{-+})$, some production from $1^-(2^{++})$ and strong production from $1^-(1^{++})$ $\bar{p}p$ atomic state. This agreement favours a 2^{++} interpretation of the AX(1565). The second argument is based on the nonobservation of the AX(1565) in the bubble chamber and in our data on S wave annihilation: a 0^{++} resonance should be produced from the $1^-(0^{-+})$ initial state without centrifugal barrier. Its nonobservation is therefore an argument against a 0^{++} assignment.

In summary we conclude that a $J^{PC}= 2^{++}$ assignment is fully compatible with the data and strongly favoured by the phase motion and by arguments based on angular momentum barrier factors in $\bar{p}p$ annihilation at rest.

The AX(1565) does not fit into one of the $q\bar{q}$ nonets. The strong production rate of the AX(1565) and the weak production rates for established $s\bar{s}$ resonances like the Φ excludes an interpretation of the AX(1565) as $f'(1525)$, since the $f'(1525)$ would need to be produced with a branching ratio of more than 50% in $\bar{p}p$ annihilation. If the AX(1565) is a $q\bar{q}$ meson, it would therefore be a radial excitation. The possible assignments are listed in Table 1. We use the spectroscopic notation: $^{2S+1}L_J$, where S is the spin of the $q\bar{q}$ system, L the intrinsic orbital angular momentum and J the total angular momentum of the resonance. The theoretical masses in Table 1 are calculated by Isgur and Weinstein [18] using a relativistic potential model. The overall agreement of their calculated masses with experimental data is very good. The experimental masses are taken from the Particle Data Group [19]. The assignment of the $f_2(1810)$ as $2\,^3P_2$ or $1\,^3F_2$ $q\bar{q}$ state is likely but not established. In any case the predicted masses of the 2^3P_2 or 1^3F_2 states are much too high to allow identification with the AX(1565). A $q\bar{q}$ interpretation for the AX(1565) would also be unlikely, if the spin of the AX(1565) is 0^{++}. It might then be the $f_0(1590)$ observed in high-energy pion–proton scattering [20]. This possibility could be tested by searching for its $\eta\eta$ and $\eta\eta'$ decay modes in the forthcoming Crystal Barrel experiment [21] at LEAR.

The AX(1565) has not been observed in reactions which are often considered to be "rich in glueballs" like radiative J/Ψ decay [22] or central production at high energies [23]. However, it may have been seen in $\bar{p}n$ annihilations into $\pi^+\pi^-\pi^-$ and $\bar{p}p$ annihilations into $\pi^0\pi^0\pi^0$ [24]. In both reactions a structure appears at a mass of 1525 MeV/c^2 and a width of 100 MeV/c^2. The authors show that the resonance cannot be the $f_2'(1525)$. But it might be the AX(1565). Note that no fit of the Dalitz plot has been made in [24], and the background is introduced as a phenomenological function. Also the $f_2(1270)$ is seen strongly, at least in $\bar{p}n \to \pi^+\pi^-\pi^-$, confirming the similar production mechanisms for the $f_2(1270)$ and the AX(1565).

The AX(1565) is produced strongly in $N\bar{N}$ annihilation. Its production rate in $\bar{p}p$ annihilation from P states is higher than the production rate of $\varrho^0(770)$, taking into account that the AX(1565) decays also in $\pi^0\pi^0$ and possibly into other final states. It is neither the $f_2'(1525)$ nor a radial excitation of the $f_2(1270)$. It is not produced in "glueball - rich" reactions. We therefore conjecture that the AX(1565) is a multiquark state, $qq\overline{qq}$ or $N\overline{N}$.

The support of the LEAR staff during the runs is gratefully acknowledged. This work was supported in part by the Deutsches Bundesministerium für Forschung und Technologie, the French Institut National de Physique Nucléaire et de Physique des Particules, the Schweizer Nationalfonds, the Österreichischer Nationalfonds and the Natural Sciences and Engineering Research Council of Canada.

We appreciate the support of Prof. Č. Zupaničič, and the continuous encouragement and active participation of Dr. R. Armenteros.

References

[1] R. Armenteros et al, "A study of $\bar{p}p$ Interactions at Rest in a H_2 Gas Target at LEAR", Proposal, CERN/PSCC 1980-101

[2] S. Ahmad et al., "Protonium Spectroscopy and Identification of P-Wave and S-Wave Initial States of $\bar{p}p$ Annihilations at Rest with the ASTERIX Experiment at LEAR", Physics at LEAR with Low-Energy Cooled Antiprotons, Eds. U. Gastaldi and R. Klapisch, Plenum Press, New York, London (1984), 109

[3] S. Ahmad et al., "($q\bar{q}$) Spectroscopy and Search for Glueballs, Baryonia and other Boson Resonances in $\bar{p}p$ Annihilations at Rest with the ASTERIX Experiment at LEAR", Physics at LEAR with Low-Energy Cooled Antiprotons, Eds. U. Gastaldi and R. Klapisch, Plenum Press, New York, London (1984), 253

[4] I.S. Shapiro, Phys. Rep. C35 (1978) 129
W.E. Buck, C.B. Dover and J.M. Richard, Ann.Phys. 121 (1979) 47
C. Amsler, Adv.Nucl.Phys. 18 (1987) 183

[5] M. Chiba et al., Phys.Lett. B177 (1986) 217; B202 (1988) 447
L. Adiels et al., Phys.Lett. B182 (1986) 405
A. Angelopoulos, Phys.Lett. B178 (1986) 441

[6] S. Ahmad et al., Phys.Lett. B152 (1985) 135

[7] R. Bizzarri et al., Nucl.Phys. B69 (1974) 307

[8] T.B. Day, G.A. Snow, J. Sucher, Phys.Rev. 118 (1960) 864
M. Leon, H.A. Bethe, Phys.Rev. 127 (1962) 636
E. Borie, M. Leon, Phys.Rev. A21 (1980) 1460
G. Reifenröther, E. Klempt, "Protonium: From Atomic Cascade to Annihilation", submitted to Nucl.Phys. A

[9] G. Reifenröther et al., Phys.Lett. B214 (1988) 325

[10] M. Ziegler et al., Phys.Lett. B206 (1988) 151
C.A. Baker et al., Nucl.Phys. A483 (1988) 631
C.W.E. van Eijk et al., Nucl.Phys. A486 (1988) 604
L. Simons, "Results from antiprotonic atoms at LEAR", in "Physics at LEAR with low energy antiprotons" eds. C.Amsler et al., Harwood Academic Publishers, Chur, London, Paris, New York, Melbourne (1988) 703

[11] M. Doser et al., Nucl.Phys. A486 (1988) 493, Phys.Lett. B215 (1988) 792

[12] R. Rückl, C. Zupancic, Phys.Lett. 150B (1985) 225
U. Schäfer et al., "X-Rays from Proton–Antiproton Annihilation into Charged Final States", Nucl.Phys. A (in print)

[13] B. May et al., "Antiproton–Proton Annihilation at Rest in H_2 into $\pi^+\pi^-\pi^0$.
I: Annihilation from S States
II: Annihilation from P States",
in preparation

[14] Ch. Zemach, Phys.Rev. B133 (1964) 1201
Ch. Zemach, Phys.Rev. B140 (1965) 97, 109

[15] S. Ahmad et al., "The ASTERIX detector", in preparation

[16] U. Gastaldi et al., "The X-ray drift chamber of the ASTERIX experiment", in preparation

[17] M. Foster et al., Nucl.Phys. B6 (1968) 107

[18] St. Godfrey and N. Isgur, Phys.Rev. D32 (1985) 189

[19] Particle Data Group, Phys.Lett. B204 (1988) 1

[20] D. Alde et al., Phys.Lett. B201 (1988) 160

[21] K. Braune et al., The Crystal Barrel: "Meson Spectroscopy at LEAR with a 4π Neutral and Charged Detector", PS 197 in: Experiments at CERN (1986)

[22] L. Köpke and N. Wermes, Phys.Rep. 174 (1989) 67

[23] F. Binon et al., Nuovo Cimento 78A (1983) 313

[24] L. Gray et al., Phys.Rev. D27 (1983) 307

Table

Meson	Calc. Mass MeV/c^2 [18]	Exp. Mass MeV/c^2 [19]	
$1\,^3P_2$	1270	1270	
$2\,^3P_2$	1820	1810	(?)
$1\,^3F_2$	2050	-	

Table 1: Comparison of calculated and observed masses of isoscalar tensor mesons.

List of Figures

1 Missing mass squared distribution of events with 2 good tracks of charged particles in coincidence with low-energy X-rays. The shaded area contains events with a probability for $\pi^+\pi^-\pi^0 > 10\%$. The probability distribution is shown as inset. 12

2 Dalitz plot of 19 735 $\pi^+\pi^-\pi^0$ events observed in coincidence with a low-energy X-ray. 13

3 $\pi^+\pi^-$ invariant mass spectrum. 14

4 Results of the Dalitz plot fits: a) $\pi^+\pi^-$ invariant mass, fit without AX(1565). b) $\pi^+\pi^-$ invariant mass, fit of reduced Dalitz plot (see text), extrapolation to high mass region. c) $\pi^\pm\pi^0$ invariant mass, extrapolation of fit of reduced Dalitz plot. d) $\pi^\pm\pi^0$ invariant mass for $\bar{p}$-GAS data. 15

5 Phase motion of the AX(1565). 16

6 Dalitz plot fit results with AX(1565) 2^{++}. 17

Figures

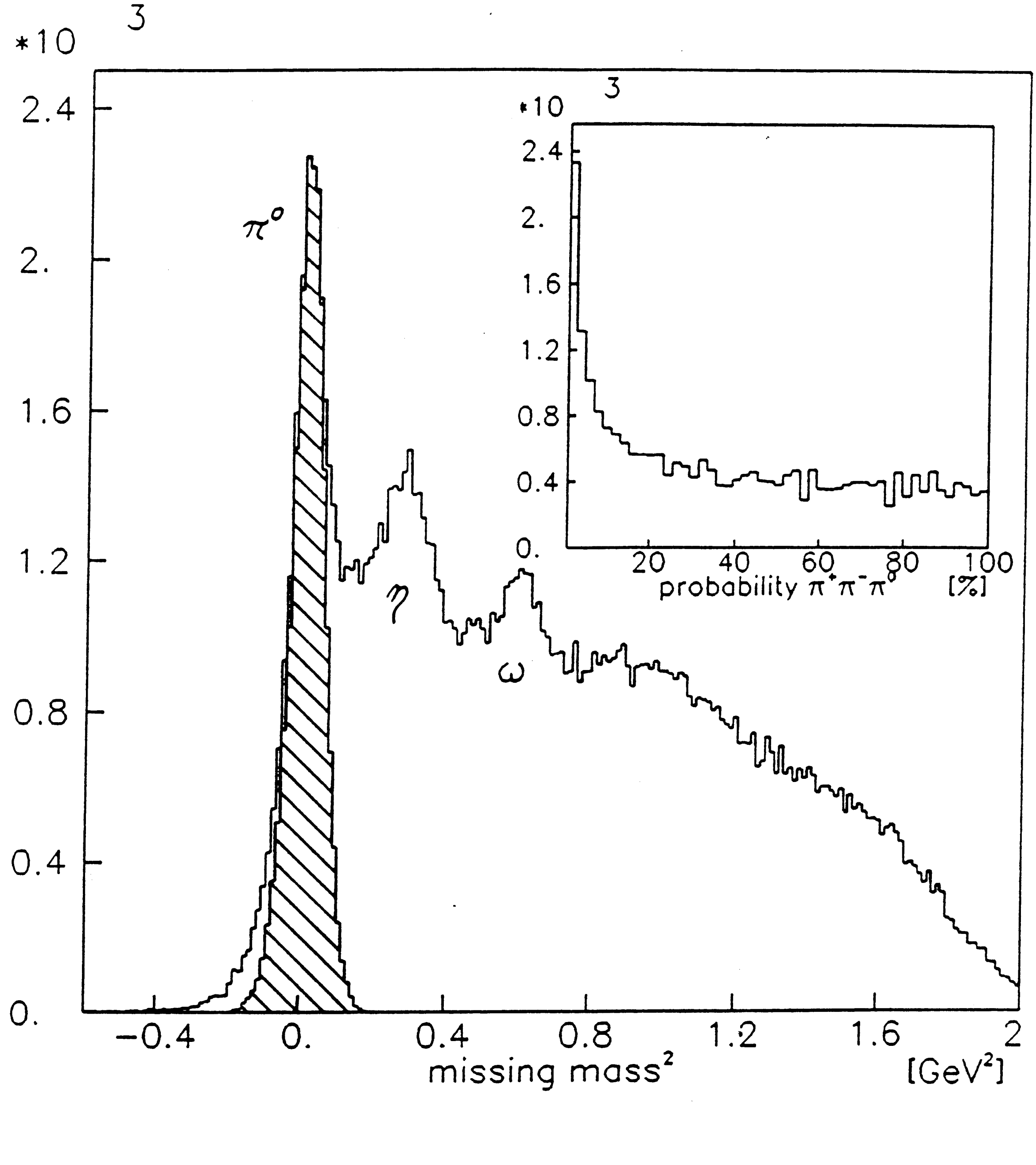

Figure 1: Missing mass squared distribution of events with 2 good tracks of charged particles in coincidence with low-energy X-rays. The shaded area contains events with a probability for $\pi^+\pi^-\pi^0 > 10\%$. The probability distribution is shown as inset.

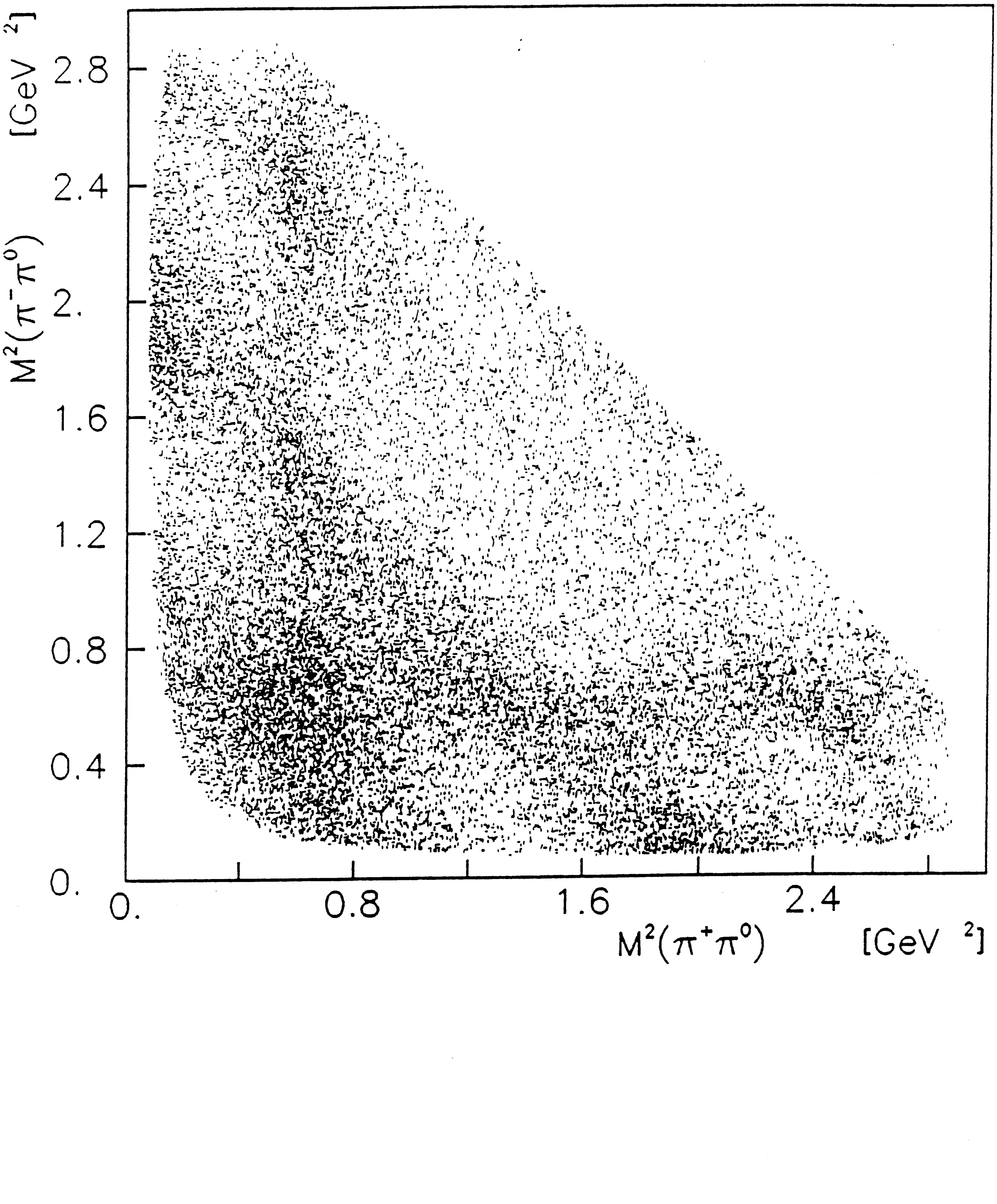

Figure 2: Dalitz plot of 19 735 $\pi^+\pi^-\pi^0$ events observed in coincidence with a low-energy X-ray.

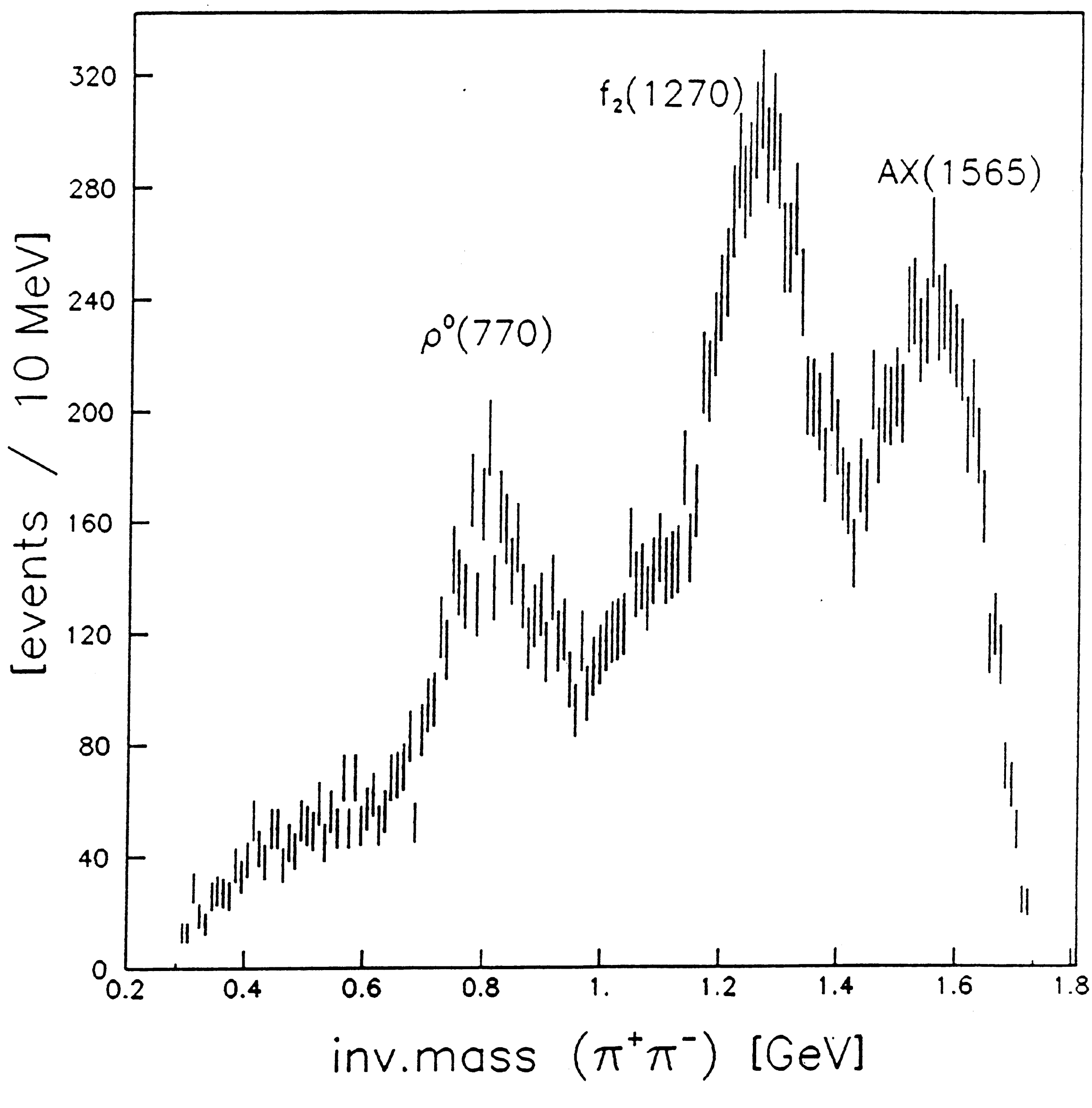

Figure 3: $\pi^+\pi^-$ invariant mass spectrum.

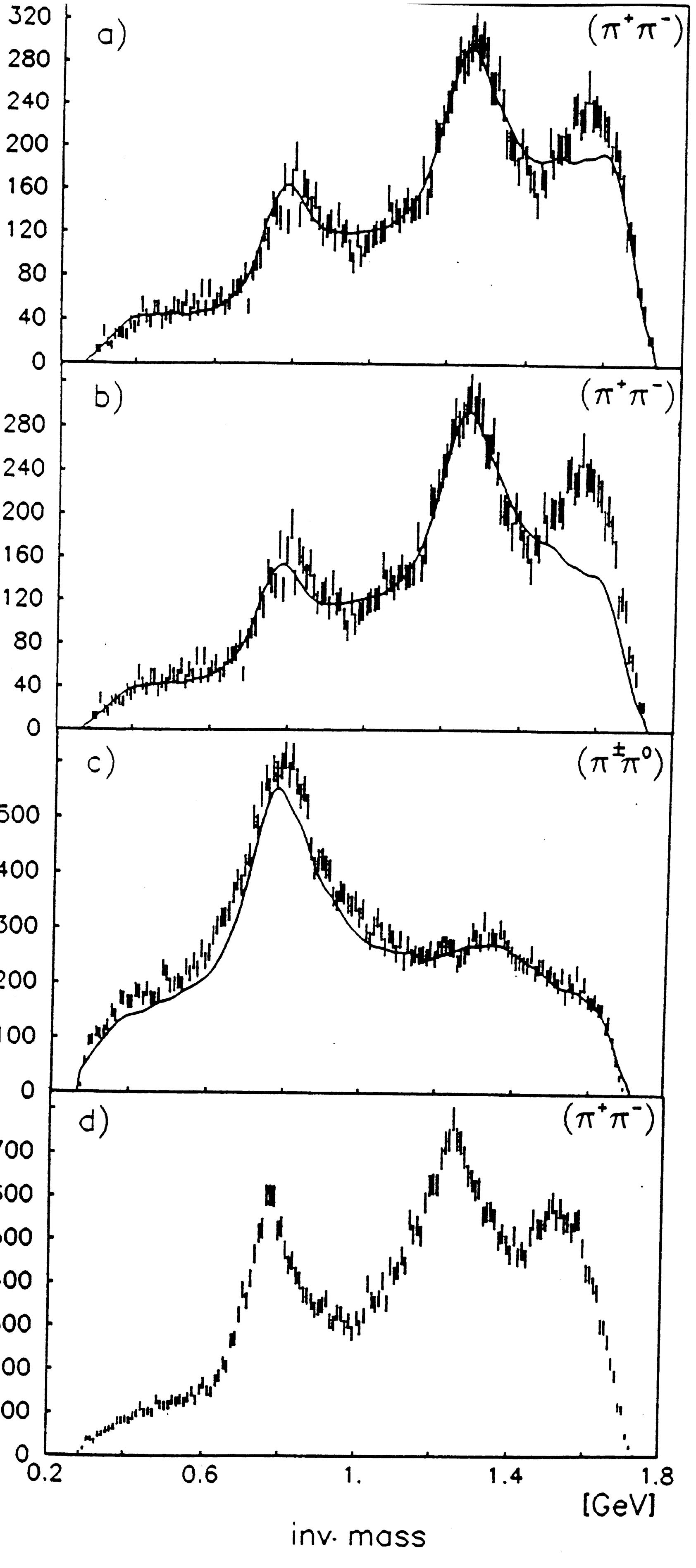

Figure 4: Results of the Dalitz plot fits: a) $\pi^+\pi^-$ invariant mass, fit without AX(1565). b) $\pi^+\pi^-$ invariant mass, fit of reduced Dalitz plot (see text), extrapolation to high mass region. c) $\pi^\pm\pi^0$ invariant mass, extrapolation of fit of reduced Dalitz plot. d) $\pi^\pm\pi^0$ invariant mass for $\bar{p}$-GAS data.

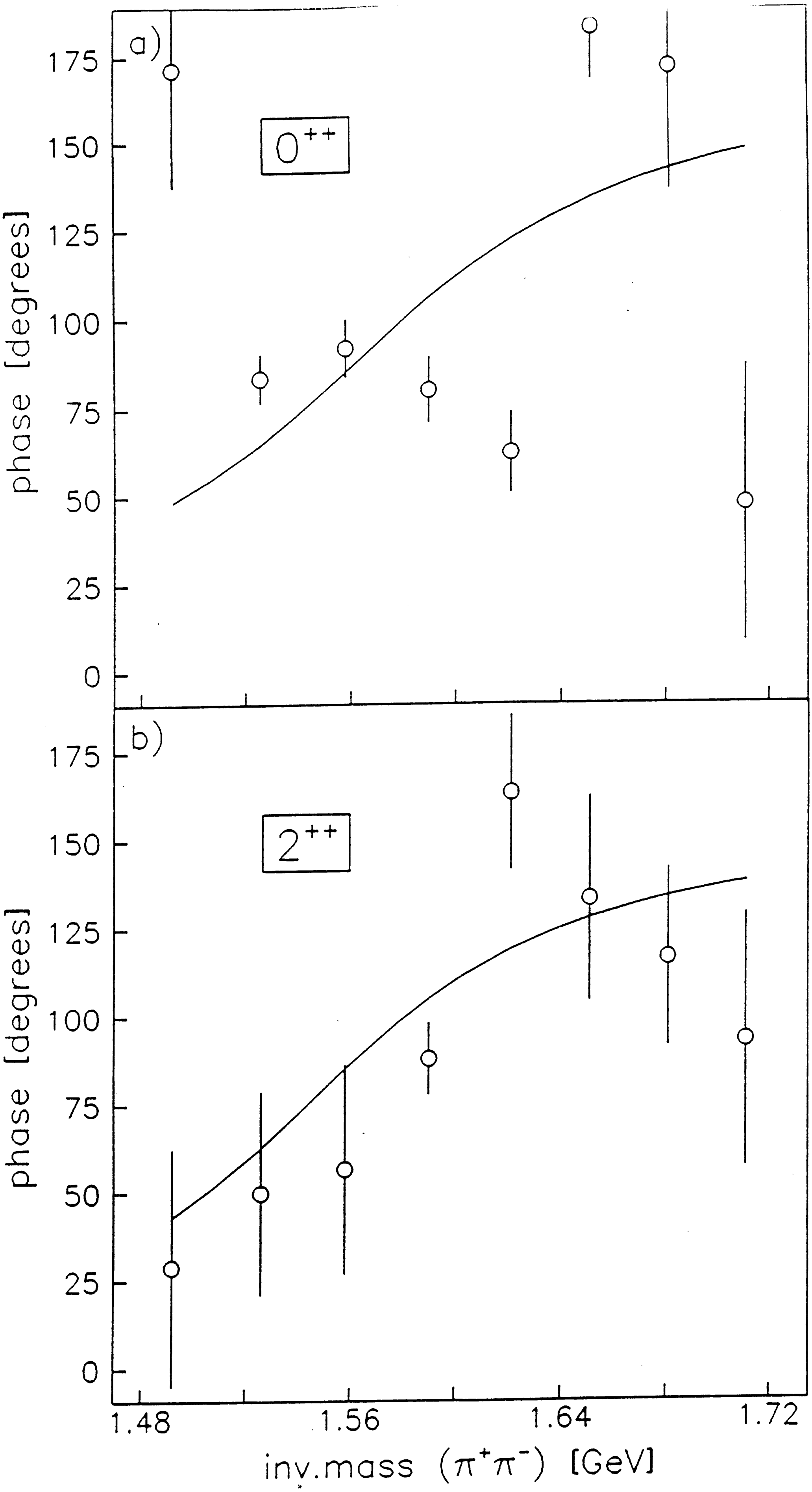

Figure 5: Phase motion of the AX(1565).

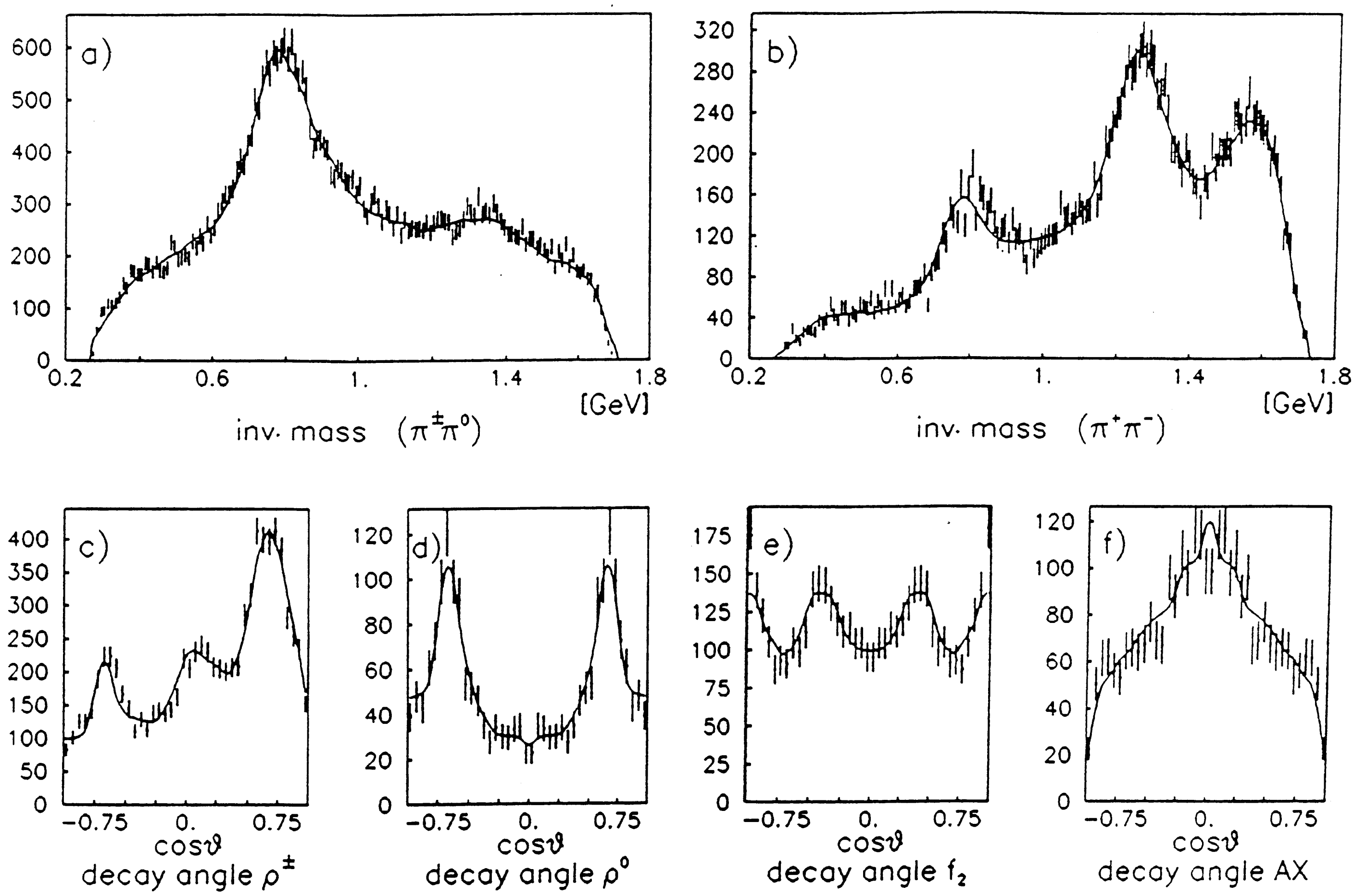

Figure 6: Dalitz plot fit results with AX(1565) 2^{++}.